Acta of Bioengineering and Biomechanics
Vol. 2, No. 1, 2000

Analysis of the velocity field of the symmetrical flow of synovial fluid in the human hip joint for the changeable gap height in the curvilinear orthogonal coordinate system

ANDRZEJ ANTONI CZAJKOWSKI

Institute of Mathematics, Mathematical & Physical Department,
University of Szczecin, Wielkopolska 15, 70-451 Szczecin,
ph. 091 489-17-17 ext. 305 or 313, e-mail: czajko@wmf.univ.szczecin.pl.
Technical University of Szczecin, Mechanical Department, Piastów 19,
70-310 Szczecin, ph. 091 449-49-47

The hydrodynamic lubrication of the human biobearing gap in the orthogonal curvilinear coordinate system is described. The axisymmetrical flow in the biobearing gap between two arbitrary rotational orthogonal curvilinear surfaces with non-monotonic generating line in the longitudinal direction and changeable height of gap is considered. As a particular case the analytical and numerical characteristics of three components of the fluid velocity vector in the circumferential, radial and meridional directions for changeable biobearing gap height is presented.

Key words: symmetrical flow of synovia, hip joint, biobearing gap

1. Introduction

The author's most recent investigations into the lubrication problem of human hip joint are shown in table 1. In comparison with [1]–[6], the new element of this paper is full numerical analysis of the synovial fluid velocity field carried out in the particular case for human hip joint.

The main aim of this paper is to present not only analytical but also complete numerical analysis of the synovial fluid velocity field for human biobearing.

Main assumptions are as follows: the rotational motion of the hip bone head, axisymmetrical and isothermic flow of synovial fluid, changeable viscosity of synovial fluid in the generating line direction, changeable height of the biobearing gap in the generating line direction, constant density of synovial fluid, two rotational orthogonal curvilinear bone surfaces with non-monotonic curvilinear sections in the longitudinal directions.

Spherical bone surfaces are considered as a particular case. Let us notice that some human joints are spherical like hip joint and humeral joint. In the human bone system, the hip joint is mostly loaded. Therefore the lubrication problem will be considered for the hip joint (figure 1).

Table 1. The problems examined in the author's papers

Synovial fluid velocity Isothermic stationary symmetrical flow of incompressible non-Newtonian synovial fluid											
Ref. No.	Joint		Gap		Generating line		Angle of lap for normal joint		Calculations		
	Hip	Humeral	Constant	Change-able	Mono-tonic	Non-mono-tonic	$\frac{\pi}{20} \div \frac{\pi}{2}$	$\frac{\pi}{20} \div \frac{19\pi}{20}$	Analy-tical	Nume-rical	Other
[1]	+		+		+		+		+	+	
[2]	+			+		+	+		+		
[3]	+			+	+		+		+	+	
[4]		+		+	+		+		+	+	
[5]	+			+	+		+		+	+	+
[6]		+		+	+		+		+	+	+
New	+			+		+		+	+	+	

Medical investigation proves that on the bone surface some roughness and some irregularities can be found. They are often caused by local deformations. In that paper, neither the above fact nor elastohydrodynamic effects are taken into account.

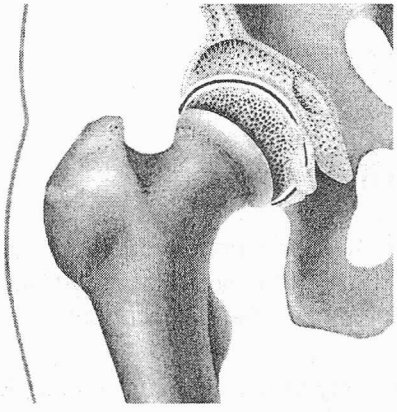

Fig. 1. Anatomical model of the human hip joint *(articulatio coxae)*

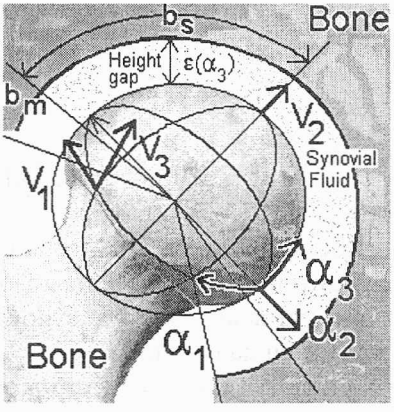

Fig. 2. Geometrical simulation of the hip joint in spherical coordinate system ($\alpha_1 = \varphi$, $\alpha_2 = y$, $\alpha_3 = \chi$)

In human joint, the rotational bone surfaces create the curvilinear biobearing gap filled with the synovial fluid. The flow of fluid is caused by rotational motion of the bone surface. For geometrical simulation let us denote: α_1 – circumferential direction,

α_2 – gap height direction and α_3 – generating line of the rotational bone direction and changeable height of gap $\varepsilon = \varepsilon(\alpha_3)$. We take into account the non-monotone generating line, which creates the right surface of bone. A typical anatomical view of the human hip joint (*articulatio coxae*) is presented in figure 1. The geometrical simulation of such a joint in the spherical coordinate system, where $\alpha_1 = \varphi$, $\alpha_2 = y$, $\alpha_3 = \chi$, is shown in figure 2. The symbols V_1, V_2, V_3 mean the components of the synovial fluid velocity vector **V**, and the symbols b_m, b_s denote the limits of lubrication. In the considerations presented, the angle of lap for normal joint ranges from $\pi/20$ to $19\pi/20$ and for the pathological joint – from $\pi/10$ to $9\pi/10$.

2. Theoretical analysis

Let us present the basic equations describing the axisymmetrical flow in biobearing gap. If the convection terms and the force of inertia are neglected, equations of conservation of momentum and equation of continuity for the stationary and incompressible synovial fluid have the following form [2]:

$$0 = -\frac{1}{h_i}\frac{\partial p}{\partial \alpha_i} + \left[\operatorname{div}\left(2\eta_p \left\| \Theta_{ij} \right\|\right)\right]_i, \tag{1}$$

$$\operatorname{div}(\mathbf{v}) = 0, \tag{2}$$

where η_p means the dynamic viscosity coefficient of the synovial fluid, **v** is the fluid velocity vector and p denotes the hydrodynamic pressure. The components of the vector $[\operatorname{div}(2\eta_p \|\Theta_{ij}\|)]$ for $i = 1, 2, 3$ have the following form:

$$\left[\operatorname{div}\left(2\eta_p \left\| \Theta_{ij} \right\|\right)\right]_i \equiv \frac{1}{h_i}\sum_{j=1}^{3}\left\{\frac{1}{h_1 h_2 h_3}\frac{\partial}{\partial \alpha_j}\left(\frac{h_1 h_2 h_3 h_i}{h_j} 2\eta_p \Theta_{ij}\right) - 2\eta_p \Theta_{jj}\frac{\partial}{\partial \alpha_i}\left(\ln h_j\right)\right\}. \tag{3}$$

Geometrical dependence of the displacement velocity components Θ_{ij} on the fluid velocity components V_i has the form:

$$\Theta_{ij} \equiv \frac{1}{2}\left[\frac{h_i}{h_j}\frac{\partial}{\partial \alpha_j}\left(\frac{V_i}{h_i}\right) + \frac{h_j}{h_i}\frac{\partial}{\partial \alpha_i}\left(\frac{V_j}{h_j}\right) + 2\delta_{ij}\sum_{k=1}^{3}\frac{V_k}{h_i h_k}\frac{\partial h_i}{\partial \alpha_k}\right] \quad \text{for } i, j = 1, 2, 3 \tag{4}$$

where h_1, h_2, h_3 are the values of the Lamé coefficients and α_1, α_2, α_3 are curvilinear orthogonal coordinates in the circumfernetial, gap height and longitudinal directions, respectively. The symbols V_1, V_2, V_3 denote the velocity components of synovial fluid in the α_1, α_2, α_3 directions.

For the axisymmetrical flow of synovial fluid, three components of the synovial fluid velocity vector depend only on the variables α_2 and α_3, the pressure function

depends only on the variable α_3 and the dynamic viscosity of synovia is independent of α_2. The height of biobearing gap is the function of the variable α_3. Neglecting the terms of the order of $Re\Psi$ and $\Psi \equiv \varepsilon \backslash a \approx 10^{-4}$, then for the layer boundary simplifications the system of equations (1)–(3) has the following form [1]–[6]:

$$0 = \frac{\partial^2 V_1}{\partial \alpha_2^2}, \tag{5}$$

$$0 = \frac{\partial p}{\partial \alpha_2}, \tag{6}$$

$$-\rho \frac{V_1^2}{h_1 h_3} \frac{\partial h_1}{\partial \alpha_3} = -\frac{1}{h_3} \frac{\partial p}{\partial \alpha_3} + \frac{\partial}{\partial \alpha_2}\left(\eta_p \frac{\partial V_3}{\partial \alpha_2} \right), \tag{7}$$

$$0 = h_1 h_3 \frac{\partial V_2}{\partial \alpha_2} + \frac{\partial}{\partial \alpha_3}(h_1 V_3), \tag{8}$$

where $0 \le \alpha_2 \le \varepsilon$, $b_m \le \alpha_3 \le b_s$, b_m and b_s mean the limits of lubrication in the α_3 direction. Moreover $h_1 = h_1(\alpha_3)$, $h_3 = h_3(\alpha_3)$, $\eta_p = \eta_p(\alpha_3)$. The centrifugal acceleration is represented by the term on the left side of equation (7). The symbols V_1, V_2, V_3 and p are the unknown functions in equations (5)–(8). The pressure values distribution counteracts the biobearing load. At the inlet of the biobearing gap the pressure has the value of the outside pressure, but in the gap it has the value of the inside pressure. The boundary conditions are as follows:

$$p = p_z \quad \text{for} \quad \alpha_3 = b_m, \tag{9}$$

$$p = p_w \quad \text{for} \quad \alpha_3 = b_s, \tag{10}$$

where p_z stands for the pressure value at the inlet of the articulation gap, p_w is the pressure value inside the biobearing gap or the pressure at the outlet of the gap. The symbols b_m and b_s mean the limits of lubrication in the α_3 direction (figure 2).

The boundary conditions for the unknown synovial fluid velocity components created by the motion of spherical bone have the following form:

$$V_1 = \omega h_1, \qquad V_2 \equiv 0, \qquad V_3 \equiv 0 \qquad \text{for} \qquad \alpha_2 = 0, \tag{11}$$

where ω IS the angular velocity of the bone. Let us notice that the bone acetabulum is motionless, therefore we have:

$$V_1 = 0, \qquad V_2 \equiv 0, \quad V_3 \equiv 0 \qquad \text{for} \qquad \alpha_2 = \varepsilon(\alpha_3), \tag{12}$$

where the function $\varepsilon = \varepsilon(\alpha_3)$ denotes some class of changeable height of the biobearing gap.

In theoretical solutions of the simplified equations (5)–(8) we take the following specifications: $x \equiv \alpha_2 \backslash \varepsilon(\alpha_3)$, $0 \le \alpha_2 \le \varepsilon$, $b_m \le \alpha_3 \le b_s$, $\eta_p = \eta_p(\alpha_3)$, $h_1 = h_1(\alpha_3)$, $h_3 = h_3(\alpha_3)$ and $\varepsilon = \varepsilon(\alpha_3)$.

•Integrating twice equation (5) with respect to the variable α_2 and accepting the condition $V_1 = \omega h_1$ for $\alpha_2 = 0$ ($x = 0$) and $V_1 = 0$ for $\alpha_2 = \varepsilon$ ($x = 1$), where the function $\varepsilon = \varepsilon(\alpha_3)$ describes the changes of the gap height, then the circumferential component of the lubricant velocity in the biobearing gap has the following form [2]:

$$V_1(\alpha_2, \alpha_3) = (1-x)\omega h_1(\alpha_3). \tag{13}$$

• Inserting the velocity component (13) into equation (7) and then integrating twice equation (7) with respect to the variable α_2 at $V_3 = 0$ for $\alpha_2 = 0$ ($x = 0$) and $V_3 = 0$ for $\alpha_2 = \varepsilon(\alpha_3)$ ($x = 1$), the longitudinal component of the lubricant velocity in the biobearing gap has the form:

$$V_3(\alpha_2, \alpha_3) = \frac{x(x-1)}{2} \frac{\varepsilon^2(\alpha_3)}{\eta_p(\alpha_3)} \frac{1}{h_3} \frac{\partial p}{\partial \alpha_3}$$

$$- \frac{x(x-1)(x^2-3x+3)}{12} \frac{\rho\omega^2 \varepsilon^2(\alpha_3)}{\eta_p(\alpha_3)} \frac{h_1}{h_3} \frac{\partial h_1}{\partial \alpha_3}. \tag{14}$$

• The longitudinal velocity component (14) is inserted into the continuity equation (8). The continuity equation is integrated once with respect to the variable α_2 in the gap height direction. Imposing the condition $V_2 = 0$ for $\alpha_2 = 0$ ($x = 0$) upon the lubricant velocity component V_2 in the gap height direction and differentiating integrals with variable limits of integration we obtain the velocity component V_2 in the following form:

$$V_2(\alpha_2, \alpha_3) = -\frac{1}{12} \frac{1}{h_1 h_3} \frac{\partial}{\partial \alpha_3} \left(x^2(2x-3) \frac{\varepsilon^3(\alpha_3)}{\eta_p(\alpha_3)} \frac{h_1}{h_3} \frac{\partial p}{\partial \alpha_3} \right)$$

$$+ \frac{1}{120} \rho\omega^2 \frac{1}{h_1 h_3} \frac{\partial}{\partial \alpha_3} \left(x^2(2x^3-10x^2+20x-15) \frac{\varepsilon^3(\alpha_3)}{\eta_p(\alpha_3)} \frac{h_1^2}{h_3} \frac{\partial h_1}{\partial \alpha_3} \right). \tag{15}$$

• The boundary condition $V_2 = 0$ for $\alpha_2 = \varepsilon$ ($x = 1$) imposed upon the velocity component (15) leads to the modified Reynolds equation which has the following form [2]:

$$\frac{\partial}{\partial \alpha_3} \left(\frac{\varepsilon^3}{\eta_p} \frac{h_1}{h_3} \frac{\partial p}{\partial \alpha_3} \right) = \frac{3}{10} \rho\omega^2 \frac{\partial}{\partial \alpha_3} \left(\frac{\varepsilon^3}{\eta_p} \frac{h_1^2}{h_3} \frac{\partial h_1}{\partial \alpha_3} \right). \tag{16}$$

• Integrating twice equation (16) with respect to the variable α_3 and imposing the boundary conditions (9)–(10), the pressure function has the following form [2]:

$$p(\alpha_3) = p_w + (p_z - p_w)\left(\int_{\alpha_3}^{b_s} \frac{\eta_p}{\varepsilon^3}\frac{h_3}{h_1}\,d\alpha_3\right)\left(\int_{b_m}^{b_s} \frac{\eta_p}{\varepsilon^3}\frac{h_3}{h_1}\,d\alpha_3\right)^{-1}$$

$$+\frac{3}{20}\rho\omega^2\left\{\left[h_1^2(b_s)-h_1^2(b_m)\right]\left(\int_{\alpha_3}^{b_s} \frac{\eta_p}{\varepsilon^3}\frac{h_3}{h_1}\,d\alpha_3\right)\left(\int_{b_m}^{b_s} \frac{\eta_p}{\varepsilon^3}\frac{h_3}{h_1}\,d\alpha_3\right)^{-1} - \left[h_1^2(b_s)-h_1^2(\alpha_3)\right]\right\}. \quad (17)$$

• Let us notice that formulae (14) and (15) contain the pressure derivative. Using formula (17) the pressure derivatives can be eliminated from formulae (14) and (15). Hence the velocity component V_2 in the gap height direction has the following form [2]:

$$V_2(\alpha_2,\alpha_3) = \frac{1}{2}(p_z - p_w)x^2(x-1)\left(\int_{b_s}^{b_m} \frac{\eta_p}{\varepsilon^3}\frac{h_3}{h_1}\,d\alpha_3\right)^{-1}\frac{1}{h_1 h_3}\frac{\partial(\ln\varepsilon)}{\partial\alpha_3}$$

$$+\frac{1}{60}\rho\omega^2 x^2(x-1)\left\{(x-1)(x-3)\,\frac{1}{h_1 h_3}\frac{\partial}{\partial\alpha_3}\left(\frac{\varepsilon^3}{\eta_p}\frac{h_1^2}{h_3}\frac{\partial h_1}{\partial\alpha_3}\right)\right.$$

$$\left.-\left[(5x^2-15x+6)\frac{\varepsilon^3}{\eta_p}\frac{h_1^2}{h_3}\frac{\partial h_1}{\partial\alpha_3} - \frac{9}{2}\left(h_1^2(b_s)-h_1^2(b_m)\right)\left(\int_{b_s}^{b_m} \frac{\eta_p}{\varepsilon^3}\frac{h_3}{h_1}\,d\alpha_3\right)^{-1}\right]\frac{1}{h_1 h_3}\frac{\partial(\ln\varepsilon)}{\partial\alpha_3}\right\}. \quad (18)$$

The velocity component V_3 in the generating line of the bone direction has the form [2]:

$$V_3(\alpha_2,\alpha_3) = \frac{1}{2}(p_z - p_w)x(x-1)\frac{1}{\varepsilon}\frac{1}{h_1}\left(\int_{\alpha_3}^{b_m} \frac{\eta_p}{\varepsilon^3}\frac{h_3}{h_1}\,d\alpha_3\right)^{-1} + \frac{3}{20}\rho\omega^2 x(x-1)\frac{1}{\varepsilon}\frac{1}{h_1}$$

$$\times\left\{\frac{\left[h_1^2(b_s)-h_1^2(b_m)\right]}{2}\left(\int_{b_s}^{b_m} \frac{\eta_p}{\varepsilon^3}\frac{h_3}{h_1}\,d\alpha_3\right)^{-1} - \frac{5x^2-15x+6}{9}\frac{\varepsilon^3}{\eta_p}\frac{h_1^2}{h_3}\frac{\partial h_1}{\partial\alpha_3}\right\}. \quad (19)$$

The above three components described by formulae (13), (18), (19) and the pressure function (17) satisfy not only basic equations (5)–(8), but also boundary conditions (9)–(12), and they tend to the known functions for the constant height of biobearing gap and monotonic generating line. In the case of ideal spherical form of

the hip bone, the curvilinear orthogonal coordinates in the latitudinal, radial and meridional directions have the following forms:

$$\alpha_1 \equiv \varphi, \quad \alpha_2 \equiv r, \quad \alpha_3 \equiv \chi, \tag{20}$$

and for the non-monotonic generating line the Lamé coefficients have the following forms:

$$h_1(\chi) \equiv R_0 \sin\frac{\chi}{R_0}, \qquad h_2 \equiv 1, \qquad h_3(\chi) \equiv 1 + O(\chi), \tag{21}$$

where R_0 is the radius of the bone head. In the case of monotonic generating line, the coefficient $h_3 \equiv 1$.

3. Numerical analysis

The parameters of the numerical analysis of the fluid velocity field are shown in table 2.

Table 2. The parameters of the numerical analysis

Numerical analysis		
Parameters	Normal joint	Pathological joint
Dimensional constants	A = 1.88307 s	A = 0.003399 s
	B = 0.00458 s^2	B = 0.00131 s^2
Dimensionless constants	A_1 = 1883	A_1 = 33
	B_1 = 4580	B_1 = 1310
Dimensionless limits of lubrication	$b_{m1} = \pi\backslash 20$	$b_{m1} = \pi\backslash 10$
	$B_{s1} = \pi\backslash 2$	$B_{s1} = \pi\backslash 2$
Dimensional synovial fluid viscosity for large (η_∞) and small (η_0) shear rates	η_∞ = 0.15 Pa·s	η_∞ = 0.007 Pa·s
	η_0 = 200 Pa·s	η_0 = 200 Pa·s
Dimensional angular velocity of the bone	$\omega = 2\ \mathrm{s}^{-1}$	
Dimensional radius of the bone	$R_0 = 25\cdot 10^{-3}$ m	
Dimensional gap height	$\varepsilon_0 = 50\cdot 10^{-6}$ m = 50 μm	
Dimensional characteristic shear rate	$\Theta_0 \equiv \frac{\omega R_0}{\varepsilon_0} = \frac{2\cdot 25\cdot 10^{-3}}{50\cdot 10^{-6}} = 1000\ \mathrm{s}^{-1}$	
	$\Theta_{b_{m1}} \le \Theta \le \Theta_{b_{s1}}$, $\quad \Theta \equiv \Theta_0 \sin(\chi_1)$	
	$A_1 = A\Theta_0$, $\quad B_1 = B\Theta_0^2$	

The circumferential (V_1), radial (V_2) and meridional (V_3) components of the synovial fluid velocity vector used in numerical analysis are presented in the following form:

$$V_1(y,\chi) = \omega R_0 V_{11}(y_1, \chi_1), \tag{22}$$

$$V_2(y,\chi) = \underbrace{\frac{(p_z - p_w)\varepsilon_0^2}{2\eta_0 R_0} V_{21p}(y_1,\chi_1)}_{V_{2p}} + \underbrace{\frac{\omega R_0 \,\mathrm{Re}\,\Psi^2}{60}\frac{\eta_\infty}{\eta_0} V_{21s}(y_1,\chi_1)}_{V_{2s}}, \tag{23}$$

$$V_3(y,\chi) = \underbrace{\frac{(p_w - p_z)\varepsilon_0^2}{2\eta_0 R_0} V_{31p}(y_1,\chi_1)}_{V_{3p}} + \underbrace{\frac{\omega\varepsilon_0 \,\mathrm{Re}\,\Psi^2}{120}\frac{\eta_\infty}{\eta_0} V_{31s}(y_1,\chi_1)}_{V_{3s}}, \tag{24}$$

$$Re \equiv \frac{\rho\omega R_0\varepsilon_0}{\eta_\infty}, \qquad \Psi \equiv \frac{\varepsilon_0}{R_0}, \qquad \chi \equiv R_0\chi_1,$$
$$y \equiv \Psi R_0 y_1, \qquad p_z = p_0 p_w, \qquad p_0 \equiv \frac{\eta_\infty^2}{\rho R_0^2 \Psi^2} \tag{25}$$

for $0 \le y_1 \le \varepsilon_1(\chi_1)$, $b_{m1} \le \chi_1 \le b_{s1}$, $b_{m1} = b_m/R_0$, $b_{s1} = b_m/R_0$.

The dimensional radial (V_{2p}) and meridional (V_{3p}) components and with the subscript p are generated by the pressure, whereas the components V_{2s} and V_{3s} with the subscript s by the motion of the bone head. The symbols η_∞, η_0 stand for the viscosity values for high and low shear rates and ε_0 is the characteristic constant value of the gap height. The values considered are in the order of: $y_1 = O(1)$, $\chi_1 = O(10)$, $\rho = O(10^3)$ [kg/m^3], $\omega = O(1)$ [1/s], $R_0 = O(10^{-3})$ [m], $\varepsilon_0 = O(10^{-5})$[m], $\Psi = O(10^{-3})$, $p_0 = O(10^2)$ [Pa], $Re = O(10^{-3})$.

The changeable viscosity of synovial fluid and the height of the gap are described by the following formulae:

$$\eta_p(\chi) = \eta_0\eta_{p1}(\chi_1), \qquad \eta_{p1}(\chi_1) = \frac{\eta_\infty}{\eta_0} + \frac{1 - \eta_\infty\eta_0^{-1}}{1 + A_1\sin\chi_1 + B_1\sin^2\chi_1}, \tag{26}$$

$$\varepsilon(\chi) = \varepsilon_0\varepsilon_1(\chi_1), \qquad \varepsilon_1(\chi_1) = 1 + 0.5\cos(\chi_1). \tag{27}$$

The dimensionless circumferential component V_{11}, radial components V_{21p}, V_{21s} and meridional components V_{31p}, V_{31s} described by the formulae (22)–(24) have the following forms:

$$V_{11}(y_1,\chi_1) = (1 - x)\sin\chi_1, \tag{28}$$

$$V_{21p}(y_1,\chi_1) = \frac{0.5x(1-x)}{\varepsilon_1^2(\chi_1)I(\chi_1)}, \tag{29}$$

$$V_{21s}(y_1,\chi_1)=x^2(x-1)^2\left[V^*(y_1,\chi_1)-V^{**}(y_1,\chi_1)\right], \tag{30}$$

$$V_{31p}(y_1,\chi_1)=\frac{0.5x(1-x)}{\varepsilon_1^2(\chi_1)I(\chi_1)}, \tag{31}$$

$$V_{31s}(y_1,\chi_1)=x(1-x)\left[\frac{18S}{\varepsilon_1(\chi_1)\sin(\chi_1)I(\chi_1)}-\frac{T(\chi_1)\varepsilon_1^2(\chi_1)\sin(2\chi_1)}{\eta_{p1}(\chi_1)}\right], \tag{32}$$

where the functions $V^*(y_1,\chi_1)$, $V^{**}(y_1,\chi_1)$, $I(y_1,\chi_1)$, $T(y_1,\chi_1)$ and the constant S are defined by the following formulae:

$$V^*(y_1,\chi_1)\equiv\frac{(x-1)(x-3)}{\sin\chi_1}\cdot\frac{X(y_1,\chi_1)-Y(y_1,\chi_1)}{\eta_{p1}^2(\chi_1)}, \tag{33}$$

$$X(y_1,\chi_1)\equiv\frac{\sin(\chi_1)\eta_{p1}(\chi_1)}{\varepsilon_1(\chi_1)}\left\{\left[1-\sin^2(\chi_1)\right]\varepsilon_1^2(\chi_1)-0.5\sin^2(\chi_1)\cos(\chi_1)\right\}, \tag{34}$$

$$Y(y_1,\chi_1)\equiv\varepsilon_1(\chi_1)\sin^2(\chi_1)\cos(\chi_1)\frac{A_1\cos(\chi_1)+B_1\sin(2\chi_1)}{\left[1+A_1\sin(\chi_1)+B_1\sin^2(\chi_1)\right]^2}\frac{(\eta_\infty-\eta_0)}{\eta_0}, \tag{35}$$

$$V^{**}(y_1,\chi_1)\equiv\frac{2.25S}{\varepsilon_1(\chi_1)I(\chi_1)}-\frac{0.5T(\chi_1)\varepsilon_1^2(\chi_1)\sin^2(\chi_1)\cos(\chi_1)}{\eta_{p1}^2(\chi_1)}, \tag{36}$$

$$x(\chi_1)\equiv\frac{y_1}{\varepsilon_1(\chi_1)},\quad I(\chi_1)\equiv\int_{b_{m1}}^{b_{s1}}\frac{\eta_{p1}(\chi_1)}{\varepsilon_1^3(\chi_1)}d\chi_1,\quad T(\chi_1)\equiv 5x^2-15x+6, \tag{37}$$

$$S\equiv\sin^2(b_{m1})-\sin^2(b_{s1}) \tag{38}$$

for $0\le y_1\le\varepsilon_1(\chi_1)$, $b_{m1}\le\chi_1\le b_{s1}$ and $b_{m1}=b_m/R_0$, $b_{s1}=b_m/R_0$.

In the numerical analysis, formulae (20)–(38) are taken into account. Numerical results are presented in figures 3–7.

Total dimensionless circumferential component V_{11} of the fluid velocity vector. Changeable gap height

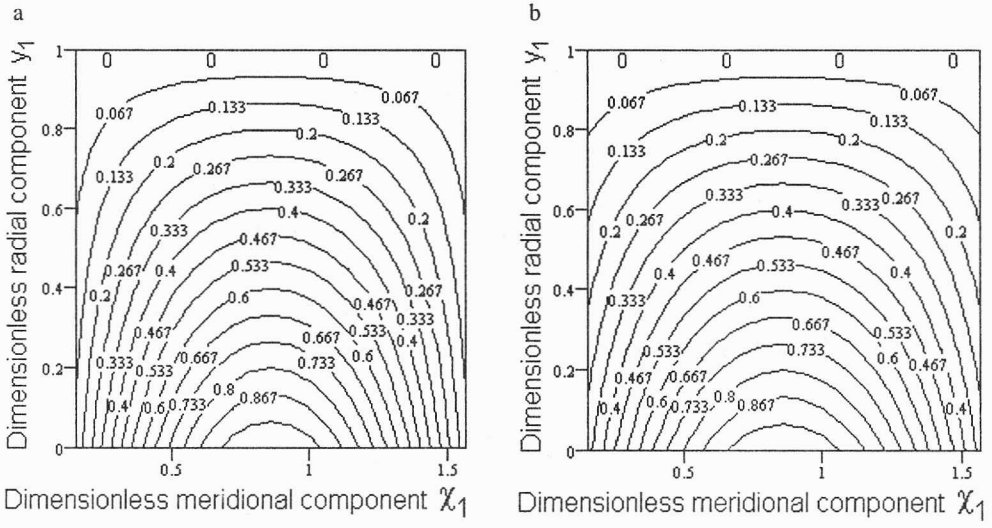

Fig. 3. The dimensionless values of the circumferential fluid velocity component V_{11}: a) normal joint, b) pathological joint. The dimensionless values of the circumferential fluid velocity vector V_{11} obtained for the constant gap height are almost the same as the values shown in the figure

Radial component V_{21p} of the fluid velocity vector caused by the pressure. Changeable gap height

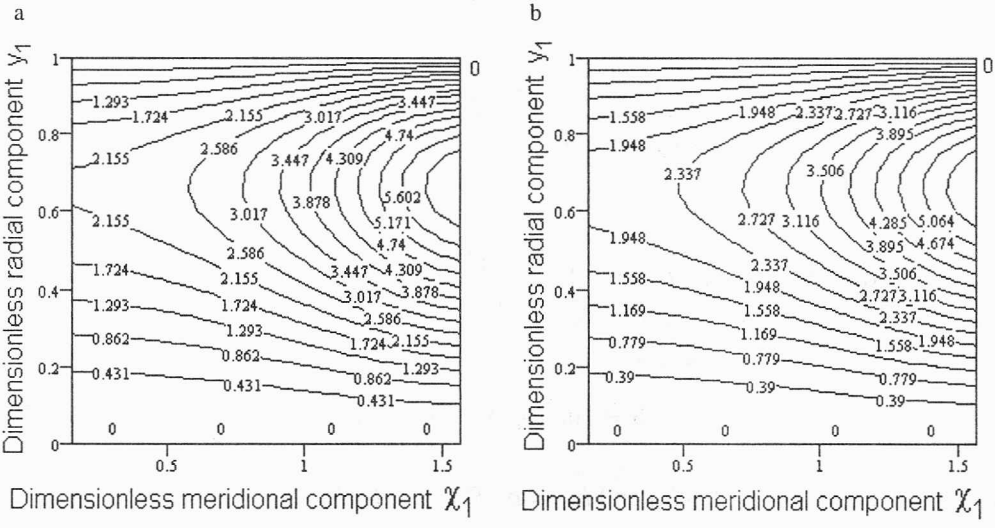

Fig. 4. The dimensionless values of the radial fluid velocity component V_{21p} caused by the pressure: a) normal joint, b) pathological joint. The dimensionless values of the radial fluid velocity vector V_{21p} are not obtained for the constant gap

Radial component V_{21s} of the fluid velocity vector caused by motion of the bone head. Changeable gap height

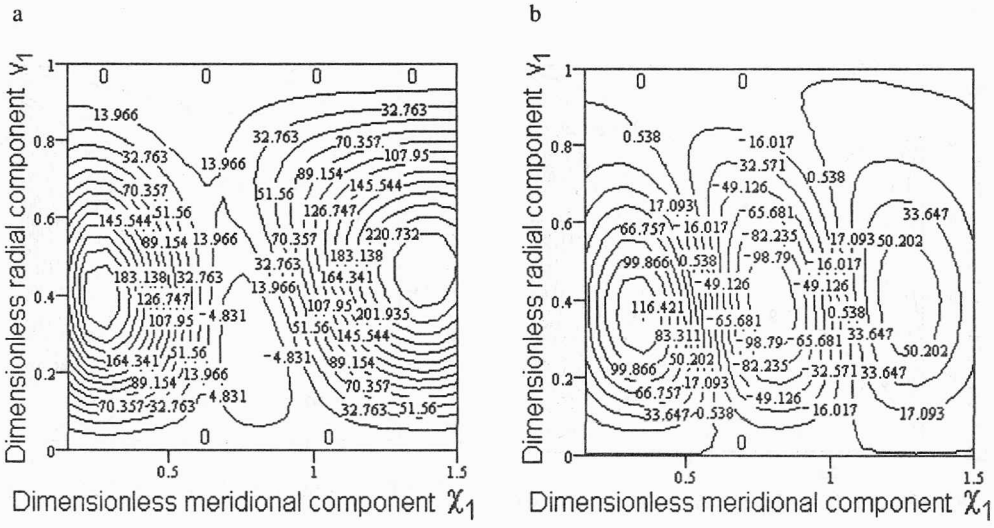

Radial component V_{21s} of the fluid velocity vector caused by motion of the bone head. Constant gap height

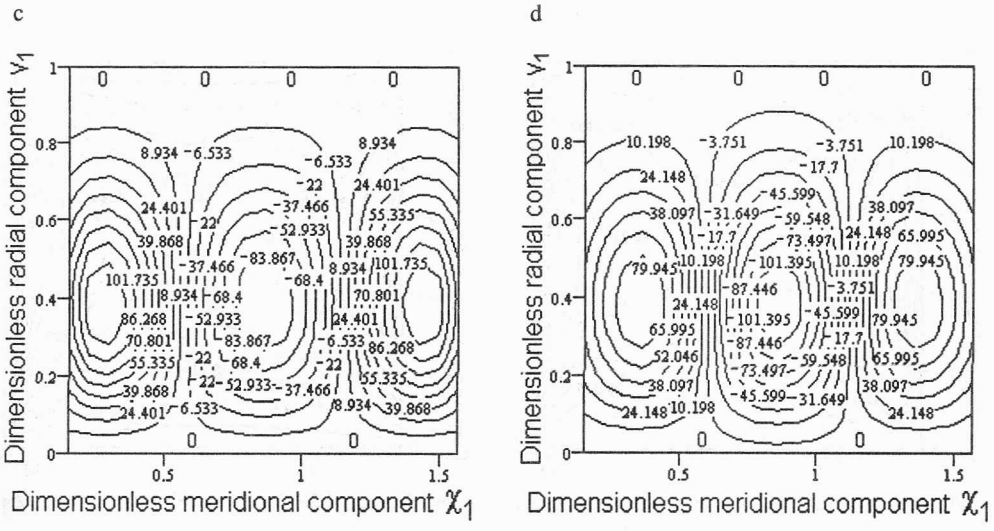

Fig. 5. The dimensionless values of the radial fluid velocity component V_{21s} caused by motion of the bone head: a) normal joint, b) pathological joint, c) normal joint, d) pathological joint

Meridional component V_{31p} of the fluid velocity vector caused by the pressure. Changeable gap height

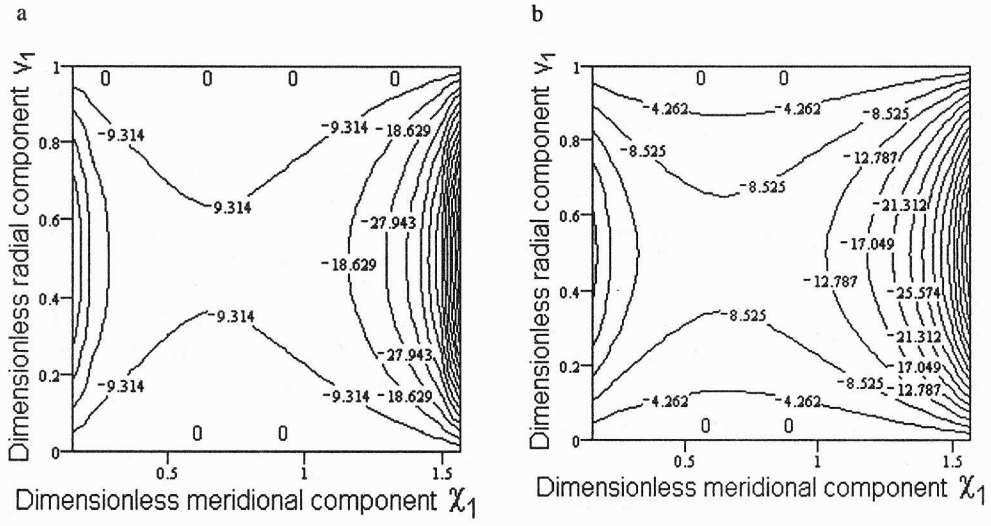

Meridional component V_{31p} of the fluid velocity vector caused by the pressure. Constant gap height

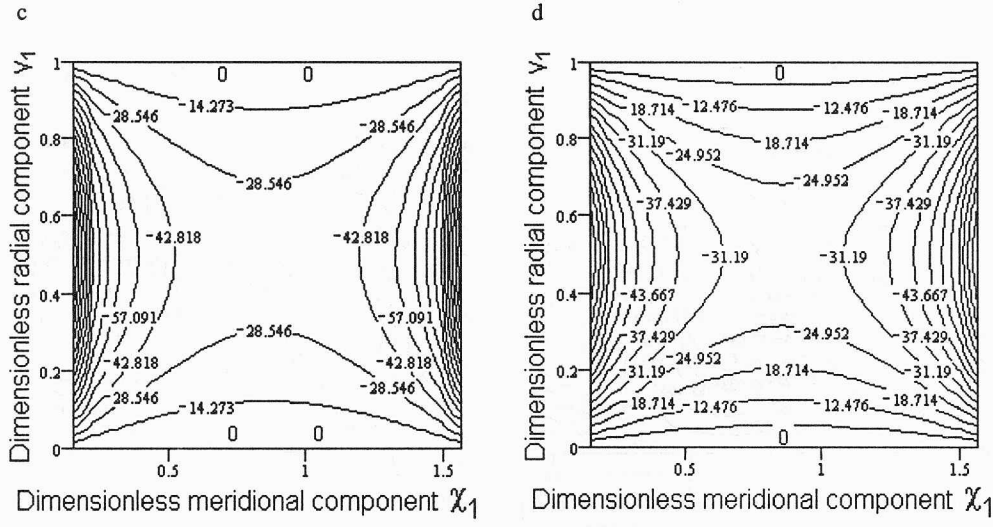

Fig. 6. The dimensionless values of the meridional fluid velocity component V_{31p} caused by the pressure: a) normal joint, b) pathological joint, c) normal joint, d) pathological joint

Meridional component V_{31s} of the fluid velocity vector caused by motion of the bone head. Changeable gap height

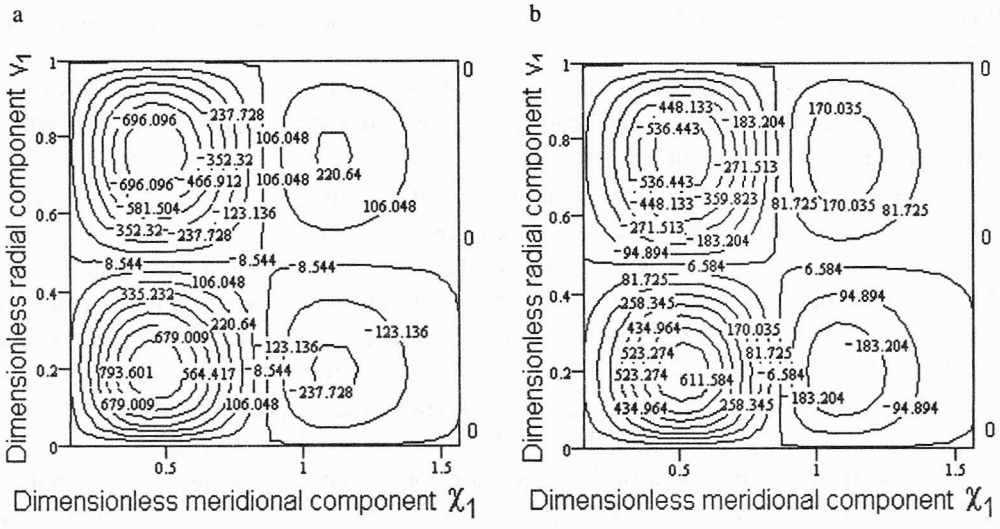

Meridional component V_{31s} of the fluid velocity vector caused by motion of the bone head. Constant gap height

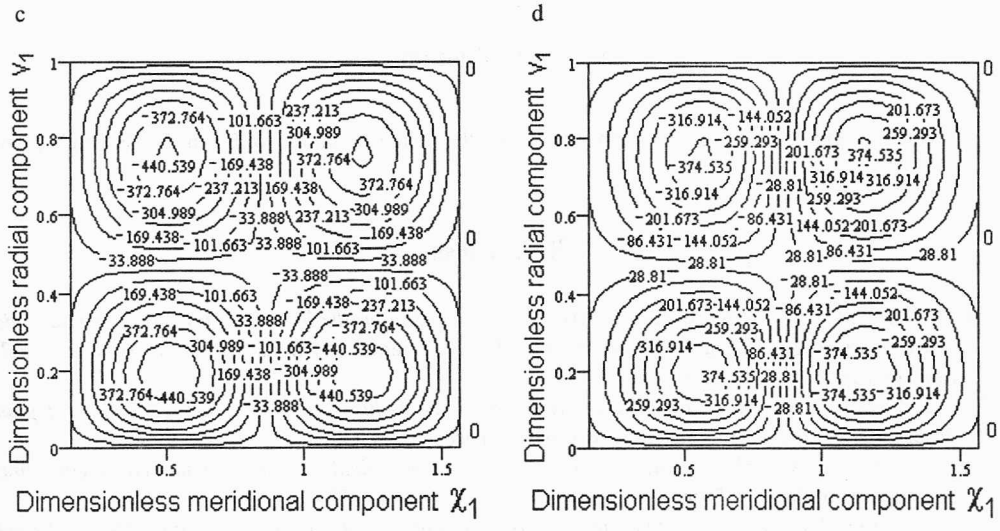

Fig. 7. The dimensionless values of the meridional fluid velocity component V_{31s} caused by the motion of the bone head: a) normal joint, b) pathological joint, c) normal joint, d) pathological joint

4. Conclusions

Based on the numerical analysis carried out for the axisymmetrical synovial fluid flow in the biobearing gap of the human hip joint, the following conclusions are drawn:

- The circumferential component values of the synovial velocity vector decrease in the radial direction from bone head to acetabulum surface. The maximum values are found in the middle of the gap height.
- The radial component of the synovia velocity vector, generated by the pressure, achieves its maximum value almost in the centre of the fluid flow area.

The radial component of the synovia velocity vector, generated by the motion of the one head, has three local extremes (one minimum and two maximum values) in the meridional direction which have two opposite signs. It means that in the rotational area the radial component changes its direction into the meridional one.

- The meridional component of the synovia velocity vector, generated by the pressure, achieves its maximum values in the centre of the fluid flow area.

The meridional component of the synovia velocity vector, generated by the motion of the bone head, has four local extremes (one–two minimum and two maximum values) in the meridional direction which have two opposite signs by pairs, respectively. It means that in the rotational area the meridional component changes its direction into the meridional one.

- All values of the velocity components of synovial fluid for the normal hip joint are higher than the values obtained for the pathological joint.

Acknowledgement

The author appreciates financial support given by the State Committee for Scientific Research, grant No. 8-T11-021-17.

References

[1] CZAJKOWSKI A.A., WIERZCHOLSKI K., *Analiza numeryczna prędkości płynu stawowego w szczelinie stawu biodrowego człowieka,* Proceedings of the 3rd Scientific Seminar *Mechanics in Medicine-3*, Rzeszów, 1996, pp. 261–269.

[2] CZAJKOWSKI A.A., *Lubrication modelling of the human hip joint with changeable height gap*, Proceedings of the 36th Symposium *Modelling in Mechanics*, Gliwice, 1997, pp. 93–98.

[3] CZAJKOWSKI A.A., *Velocity calculations of synovia symmetrical flow in the changeable gap joint,* Proceedings of the 37th Symposium *Modelling in Mechanics*, Gliwice, 1998, pp. 65–70.

[4] CZAJKOWSKI A.A., *Velocity calculations of synovia symmetrical flow for the changeable gap height of the human humeral joint*, Abstracts of the 9th International Symposium *System-Modelling -Control-9*, Zakopane, 1998, pp. 27/1–27/6.

[5] CZAJKOWSKI A.A., *Przykłady obliczeń prędkości cieczy synowialnej w szczelinie stawu biodrowego człowieka,* Proceedings of the 4th Scientific Seminar *Mechanics in Medicine-4*, Rzeszów, 1998, pp. 69–77.

[6] CZAJKOWSKI A.A., *Particular calculations of synovial fluid velocities in the gap of human humeral joint*, Exploitation Problems of Machines, 1998, Vol. 33, No. 2 (114), pp. 315–232.

[7] DOWSON D., *Bio-tribology of natural and replacement synovial joints*, Vol. 2, [In:] Van Mow C., Ratcliffe A., Woo S.L-Y., *Biomechanics of diarthrodinal joint*, Springer-Verlag, New York, Berlin, London, Paris, Tokyo, Hong Kong, 1990, Vol.2, pp. 305–345.

[8] FERZIGER J.H., PERIĆ M., *Computational methods for fluid dynamics,* Springer-Verlag, New York, Berlin, London, Paris, Tokyo, Hong Kong, 1996.